Sensors & Actuators: B. Chemical 441 (2025) 137962

Contents lists available at ScienceDirect

Sensors and Actuators: B. Chemical

journal homepage: www.elsevier.com/locate/snb

A dual colorimetric-electrochemical platform based on bromocresol green for the selective detection of atropine

Larissa M.A. Melo [a,b,1], Elena Bernalte [a,1], Robert D. Crapnell [a], Rodrigo M. Verly [b], Rodrigo A.A. Muñoz [c], Wallans T.P. dos Santos [b,d,*], Craig E. Banks [a,**]

[a] Faculty of Science and Engineering, Manchester Metropolitan University, Dalton Building, Chester Street, Great Britain, M1 5GD, United Kingdom
[b] Department of Chemistry, Federal University of Vales do Jequitinhonha and Mucuri, Campus JK, Diamantina, Minas Gerais 39100000, Brazil
[c] Institute of Chemistry. Federal University of Uberlândia, Uberlândia, Minas Gerais 38400-902, Brazil
[d] Department of Pharmacy, Federal University of Vales do Jequitinhonha and Mucuri, Campus JK, Diamantina, Minas Gerais 39100000, Brazil

ARTICLE INFO

Keywords:
Bromocresol green
Atropine
Colorimetric
Electrochemical
Forensic analysis

ABSTRACT

Atropine is crucial in forensic investigations due to its role in poisoning cases, requiring precise detection methods. We propose a novel dual-mode analytical platform that combines screen-printed graphite electrodes with square-wave voltammetry and a colorimetric reaction using bromocresol green. This dual platform provides three distinct analytical responses: a colour change via the colorimetric reaction and electrochemical responses before and after the colorimetric reaction, allowing robust atropine identification. For the first time, the electrochemical behaviour of atropine in the presence of bromocresol green has been investigated, with mechanistic insights elucidated through NMR analysis. Although atropine alone undergoes an irreversible oxidation process, the colorimetric reaction facilitates a redox process involving bromocresol green, allowing indirect atropine detection. The real-world applicability of this dual-sensing platform is demonstrated by detecting atropine in drink and biological samples for potential spiking and poisoning diagnosis. Importantly, the platform is shown to function within solutions containing quinine, proving its suitability to analysing strong and bitter tonic water drink with low atropine concentrations, overcoming this known analytical problem. The developed method exhibited a wide linear range (0.001–0.4 mg mL^{-1}), a low limit of detection (0.255 μg mL^{-1}), and excellent stability with relative standard deviation lower than 7 %. Interference studies confirm the method's selectivity, and atropine recoveries from drink and biological samples were close to 100 %. The proposed platform is a simple, rapid, and selective screening tool, and shows significant potential for forensic applications in atropine detection.

1. Introduction

Atropine is a tropane alkaloid derived from plants in the *Solanaceae* family, such as *Atropa belladonna* (deadly nightshade) and *Datura stramonium* (jimson weed) [1]. Atropine is frequently used in medical settings, as an antidote for organophosphate poisoning, to treat bradycardia and gastro-intestinal spasms, and in ophthalmology to dilate the pupils (mydriasis) [2–5]. In therapeutic amounts, atropine is safe and effective, but in excessive doses, it can cause serious symptoms such as hallucinations, agitation, tachycardia, hyperthermia, urinary retention, dry skin, and, in extreme cases, coma and death [6–8]. Due to these toxic properties at high doses, atropine has been reported in assassination attempts [9–12].

In a forensic context, identifying atropine at toxic levels in the victim's body is crucial for determining the cause of intoxication and assisting in immediate treatment. Accurate toxicological analyses can detect atropine in blood, serum and plasma, providing direct evidence of poisoning [13–15]. However, traditional laboratory methods such as high-performance liquid chromatography and mass spectrometry, despite offering high precision, require significant time and skill for

* Corresponding author at: Department of Chemistry, Federal University of Vales do Jequitinhonha and Mucuri, Campus JK, Diamantina, Minas Gerais 39100000, Brazil.
** Corresponding author.
E-mail addresses: wallanst@ufvjm.edu.br (W.T.P. dos Santos), c.banks@mmu.ac.uk (C.E. Banks).
[1] These authors contributed equally

https://doi.org/10.1016/j.snb.2025.137962
Received 25 January 2025; Received in revised form 6 May 2025; Accepted 11 May 2025
Available online 12 May 2025

sample collection and processing [16]. In this context, electroanalytical approaches emerge as promising alternatives, providing rapid and sensitive on-site detection, which is essential for rapid intervention [17–20]. These methods are vital for identifying atropine in cases of poisoning, as illustrated in a recent review [9].

Electroanalytical methods have been used to detect atropine, employing techniques such as electrochemiluminescence [21] and various forms of voltammetry, including linear and cyclic voltammetry [22,23], differential pulse and square-wave voltammetry [24–27] and adsorptive anodic stripping voltammetry [28]. Most reported methods use modified electrodes to achieve selective atropine analysis, except Ramdani et al. [23] Arantes et al. [20], and João et al. [27], which utilised screen-printed electrodes and 3D-printed electrodes, respectively. Although modified electrodes provide selectivity, they add an additional step to the overall methodology, often compromises their reproducibility and increase the overall cost of the procedure [29]. Forensic laboratories in developing or underdeveloped countries often lack the infrastructure for complex and high-cost analyses [30–32]. Therefore, simpler and low-cost methods are highly desirable in real forensic scenarios.

Due to the bitter taste of atropine, it is typically mixed into strongly flavoured drinks to mask its bitter taste, increasing the need for accurate and selective analytical methods to detect atropine in this scenario [12,33]. Yet, there are no official screening methods for the detection of this compound, particularly in biological samples and beverages such as tonic water, where the overlapping oxidation signals of atropine and quinine present significant challenges in the selective electroanalytical detection [9,34]. Therefore, the development of unique and advanced electrochemical detection techniques is essential to overcome these real-world challenges in forensic investigations.

In this context, we propose the use of screen-printed graphite electrodes (SPE-Gr) combined with a colorimetric method using bromocresol green as a dual-mode sensor to detect atropine in drinks and biological samples. The proposed method provides three distinct analytical responses: (1) the electrochemical behaviour prior to the colorimetric reaction; (2) the colour change resulting from the reaction with bromocresol green; and (3) the electrochemical behaviour after the colorimetric reaction. This approach offers a more robust and accurate analytical response for identifying and quantifying atropine, even in the presence of other active substances, making it applicable in real forensic scenarios.

2. Experimental section

2.1. Chemicals

All solutions were prepared with deionised water of resistivity not less than 18.2 MΩ cm from a Milli-Q Integral 3 system from Millipore UK (Watford, UK). The atropine and bromocresol green analytical standards were purchased from Tokyo Chemical Industry (Oxford, UK), atropine was solubilised in methanol and bromocresol green was prepared at 1 mg mL^{-1} in aqueous solution with 5 % methanol. The stock solutions (5 mg mL^{-1}) of atropine were diluted (10-times) in a supporting electrolyte for electrochemical measurements before and after reaction with bromocresol green. Electrochemical studies of atropine and bromocresol green were conducted in a Britton-Robinson buffer solution (0.1 mol L^{-1}), composed of an equimolar mixture of boric, phosphoric, and acetic acids. The pH was adjusted (2−12) using 1 mol L^{-1} NaOH. Borate and carbonate buffer solutions (0.1 mol L^{-1}) were also evaluated as supporting electrolytes, as well as different concentrations (0.05, 0.1 and 0.2 mol L^{-1}) of borate buffer were studied to verify the influence of ionic strength on the atropine detection in the presence of bromocresol green. Uric acid (UA), citric acid (CA), ascorbic acid (AA), caffeine (CAF), glucose (GLU) and fructose (FRU) were evaluated as potential interferents for atropine detection by the proposed method. All reagents were of analytical grade and were purchased from Sigma-Aldrich (Lancashire, United Kingdom).

Synthetic urine was prepared as described by Laube et al. [35], artificial saliva as described by Qian et al. [36], and artificial vitreous humour as described by Thakur et al. [37]. Synthetic/artificial biological samples, along with samples of gin, whiskey, tonic water, energy drink, and gin with tonic water, were spiked with 2.5 mg mL^{-1} of atropine for analysis.

2.2. Instrumental and apparatus

A PGSTAT 204 potentiostat (Metrohm Autolab BV, Utrecht, Netherlands) controlled by NOVA 2.1 software was used to perform the voltammetric experiments, while a portable Sensit BT dual-channel potentiostat controlled by PSTrace 5.8 software on a mobile phone was used as a proof of concept for in-situ analyses. The electrochemical behaviour of atropine and bromocresol green was characterised using screen-printed graphite electrodes (SPE-Gr) produced in the laboratory, featuring a 0.07 cm^2 graphite working electrode, a graphite auxiliary electrode, and an Ag/AgCl reference electrode. All electrochemical analyses were performed using only the SPE pseudo-reference (vs. Ag/AgCl).

2.3. Nuclear magnetic resonance (NMR)

Nuclear Magnetic Resonance (NMR) experiments were conducted on a Jeol-JNM-ECZ500R/S3 500 MHz spectrometer (JEOL Ltd., Tokyo, Japan). One-dimensional spectra of 1 H or 13 C were acquired for the following samples diluted in 1 mL of methanol-d4: (i) bromocresol green (1 mg mL^{-1}); (ii) atropine (5 mg mL^{-1}); (iii) reduced bromocresol green product (R_1 at − 0.85 V) (0.02 mg mL^{-1}); (iv) bromocresol green and atropine (4.2 mg mL^{-1}) solution (1:12, mol:mol); (v) reduced product from bromocresol green and atropine (0.42 mg mL^{-1}) solution (R_1) (1:12, mol:mol).

^{1}H spectra were acquired using the single_pulse_wet.jxp pulse program for field homogenization (shimming) and to determine the irradiation frequency of the water signal (o1), 20 ppm spectra width, 65536-time domain (TD) points and 512 scans. ^{1} ^{3}C spectra were acquired using carbon.jxp pulse program, 200 ppm spectra width, 32768 TD and 2048 scans. All one-dimensional ^{1}H and ^{1} ^{3}C experiments were processed using Delta 6.1.0 software (JEOL Ltd., Tokyo, Japan).

2.4. Electrochemical measurements

Before each measurement, the SPE-Gr was electrochemically conditioned using a pH 9 borate buffer solution for 5 successive scans in the potential window of −0.4 V to + 0.6 V (vs. Ag/AgCl). The electrochemical studies were performed using cyclic voltammetry on a SPE-Gr with different scan rates and pH values. Square-wave voltammetry and differential pulse voltammetry were employed, and atropine detection was optimised using the square-wave voltammetry technique with a SPE-Gr. The optimal parameters were obtained with 50 mV amplitude, 10 mV step potential and 10 Hz frequency. Voltammograms obtained by square-wave voltammetry underwent background subtraction using polynomial fit in OriginPro 2016 software. Electrochemical measurements were conducted before and after the colorimetric reaction with bromocresol green.

2.5. Colorimetric process

The colorimetric reaction was performed using clear spot tests by mixing 100 μL of a stock solution of atropine at 5 mg mL^{-1} or methanol (blank) with 20 μL of a bromocresol green solution (1 mg mL^{-1} prepared in an aqueous solution containing 5 % methanol). A yellow color indicated the absence of atropine, as observed in the negative control (methanol), while a color change to green indicated the presence of atropine. The color change visible to the naked eye was used as a

screening method for the presence of atropine in beverage and biological samples, with subsequent electrochemical analysis performed to confirm and quantify the analyte. After the colorimetric reaction, a 10 μL aliquot was taken and diluted tenfold in borate buffer solution (90 μL, 0.05 mol L^{-1}, pH 9) for electrochemical measurement.

3. Results and discussion

The development of analytical platforms capable of producing reliable, validated, and on-site analysis is vital in a wide range of applications, in particular within forensic investigations. As such, dual method analytical platforms offer significant promise with colorimetric and electroanalytical techniques offering excellent synergy.

A combined analytical approach integrating three sequential responses—initial electrochemical screening, a colorimetric test, and a confirmatory electrochemical analysis post-colorimetric reaction—was employed for the detection of atropine in forensic-relevant samples such as adulterated beverages and biological fluids. This strategy enhances the reliability and selectivity of the analysis by leveraging the complementary advantages of each technique: rapid and sensitive detection by electrochemistry, straightforward visual interpretation through colorimetry, and confirmatory quantification with improved selectivity using electrochemical analysis after sample treatment. The use of multiple analytical responses allows cross-validation of results, reducing the likelihood of false positives or negatives, which is critical in forensic investigations where analytical certainty is essential. This multiparametric method provides a robust and practical solution for on-site or preliminary laboratory screening of atropine in complex matrices.

3.1. Colorimetric reaction and electrochemical analyses

First, the colorimetric reaction between bromocresol green and atropine was explored and optimised using 100 μL of atropine standard solution (5 mg mL^{-1}) or methanol (as a blank) and 20 μL of bromocresol green solution. A yellow colour was observed in the absence of atropine, while a colour change to green indicated the presence of atropine. For real-world applicability, the stability of this colour change is vital to avoid false results and was therefore assessed at various exposure times to sunlight: 0 s, 30 s, 1 min, 3 min, 5 min, 10 min, 15 min, 20 min, 25 min, and 30 min, as shown in Figure S1. It can be seen that the colour remained stable without any changes during the exposure times studied, indicating its applicability to real-world analysis no matter the time of day. Electrochemical studies were then explored systematically in two stages: before and after the colorimetric reaction, with the subsequent electrochemical responses evaluated as described in Scheme 1.

The methodological strategy outlined in Scheme 1 provides three distinct analytical responses: the electrochemical behaviour before the colorimetric reaction, the colour change from the colorimetric reaction, and the electrochemical behaviour after the colorimetric reaction. This robust approach enables the on-site identification of atropine in forensic samples using portable equipment such as a cellphone and a portable potentiostat for user-friendly and easy interpretation, contributing to real forensic in-situ screening analyses. A photograph of the materials used during the analyses is presented in Figure S2.

3.2. Study of the electrochemical behaviour of bromocresol green and atropine

The electrochemical behaviour of atropine was then evaluated in 0.1 mol L^{-1} Britton-Robinson buffer solution across a pH range from 2 to 12, both in the absence (a) and presence (b) of bromocresol green, using cyclic voltammetry on SPE-Gr, as shown in Fig. 1 atropine exhibits an irreversible oxidation process (P_{ATP}) on SPE-Gr (Fig. 1a) that also appears in the presence of bromocresol green together with the two quasi-reversible redox pairs (O_1/R_1 and O_3/R_2) and one irreversible oxidation (O_2) corresponding to bromocresol green (Fig. 1b). The O_2 and R_1 processes are observed at all pH levels from 2 to 11, while O_1, O_3 and R_2 are only seen at pH values less than 6, with P_{ATP} only observed at pH values above 6 (Fig. 1a and Fig. 1b).

A pH-dependent behaviour of the redox processes of atropine and bromocresol green on the SPE-Gr was also observed since the peak potentials (E_p) of these electrochemical processes were shifted to more negative potentials with increasing pH. Figure S3a and Figure S3b show plots of E_p *vs.* pH of the redox processes occurring on the SPE-Gr and the linear ranges observed are summarised in Table S1. The slopes obtained for the pH dependence of the O_1/R_1 and O_3/R_2 redox couples are close to the theoretical value of 0.0592 V/pH, indicating that equal numbers of electrons and protons are involved in these reversible redox processes. The difference in the behaviour of E_p *vs.* pH observed for P_{ATP} at pH values above 9 is attributed to the pK_a of this molecule (9.19). The same

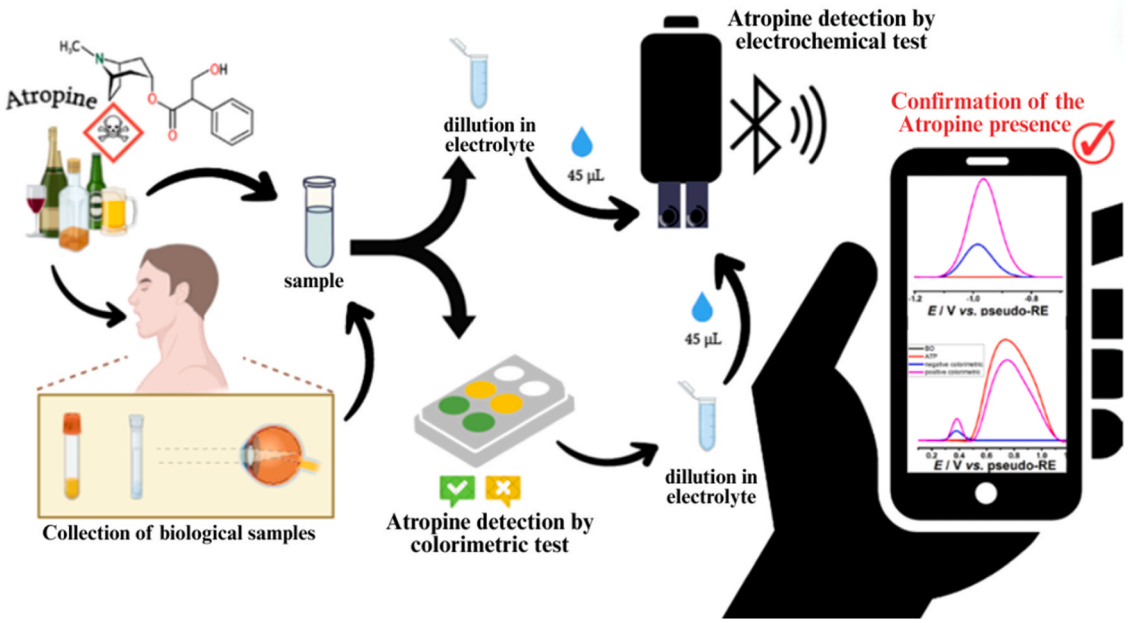

Scheme 1. Schematic model of the proposed method used for atropine detection in biological and drinks samples.

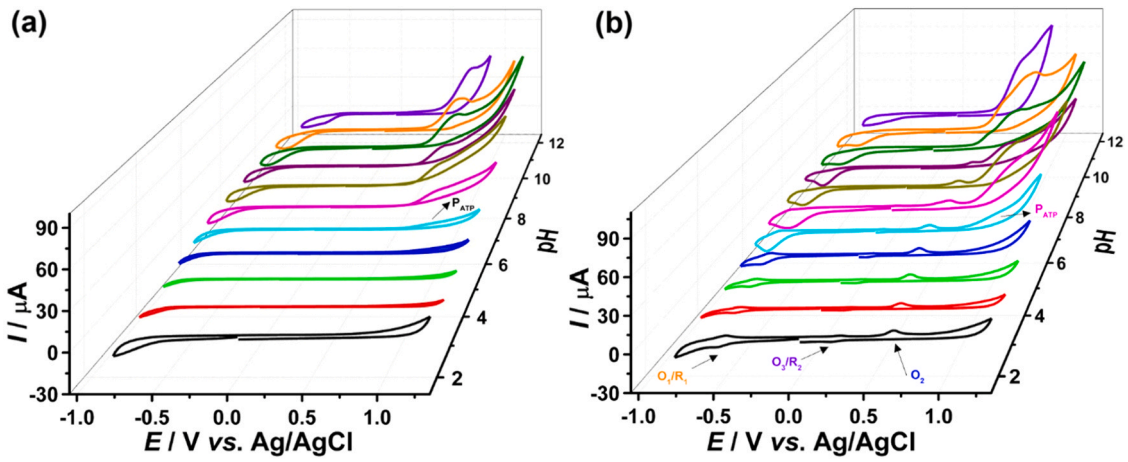

Fig. 1. 3D plots of recorded cyclic voltammograms (first scan) of 0.5 mg mL^{-1} atropine in 0.1 mol L^{-1} Britton-Robinson buffer solution with different pH values (from 2–12) in absence (**a**) and presence of the bromocresol green (**b**). All potential scans started at 0.0 V (*vs.* Ag/AgCl), with a scan rate of 50 mV s^{-1}. P_{ATP}: irreversible oxidation process of atropine (black). O_1/R_1 (orange) and O_3/R_2 (purple): quasi-reversible redox process of bromocresol green, and O_2 (blue) irreversible oxidation process of bromocresol green.

trend is observed in the case of bromocresol green ($pk_a = 6.57$) for the O_1/R_1 redox process at pH values above 6. Furthermore, at pH values above 7, there is better correlation with the peak current (I_p), providing an adequate response for the detection of atropine, as observed for the P_{ATP}, O_2 and R_1 processes (Figure S3a and Figure S3c). Therefore, pH 9 was chosen for atropine detection due to its good sensitivity and well-defined peaks for the O_2, P_{ATP} and R_1 processes. Subsequently, different buffer solutions at the selected pH were evaluated as supporting electrolytes. The results obtained using Britton-Robinson, borate, and carbonate-bicarbonate buffers are presented in Figure S4. Although no significant differences in peak current were observed between the Britton-Robinson and borate buffers at pH 9, the borate buffer was selected as the supporting electrolyte due to its simpler preparation compared to the Britton-Robinson buffer. Under these conditions, various borate concentrations were tested to evaluate the influence of ionic strength. A concentration of 0.05 mol L^{-1} was chosen for providing excellent resolution of the redox processes, as assessed by the ratio of peak current to peak width at half height (Figure S5). These optimisations aimed to achieve adequate peak current while maintaining a narrow peak profile, thereby minimizing overlaps with other electroactive species.

Cyclic voltammetry at different scan rates (ν) were used to evaluate the mass transport control of the redox reactions observed on the SPE-Gr surface in 0.05 mol L^{-1} borate buffer solution at pH 9 (Figure S6). The I_p of atropine (P_{ATP} - black dots and Figure S6a) and bromocresol green (R_1 - orange dots and Figure S6b, O_2 - blue dots and Figure S6c) on SPE-Gr were more proportional to the square root of the scan rate (Figure S6e) than to the scan rate itself (Figure S6d), indicating that the mass transport during the electrochemical processes is predominantly controlled by diffusion on the SPE-Gr surface. The logarithmic plots of I_p *vs.* ν show linear relationships (Figure S6f), with equations described in Table S2, displaying slopes ≤ 0.5 that confirm diffusion control, except for R_1 (slope = 0.6) indicating a mixed diffusion and adsorption-controlled process.

It can also be observed that, in the presence of atropine, an oxidation process forming a quasi-reversible redox couple with R_1 is favoured at high scan rates, indicating that this process most likely presents fast reaction kinetics (Figure S6). On the contrary, in the absence of atropine (negative colorimetric reaction) only a lower intensity reduction process is observed, as demonstrated in Figure S7 a-d. The linear equations for all the redox processes described are shown in Table S2. It is worth mentioning that after the colorimetric reaction with atropine, the slope of the linear regression for R_1 changes, being greater after colorimetric reaction (0.60–0.65). This indicates that the diffusion coefficient of bromocresol green decreases, suggesting that the bromocresol green molecule could undergo structural changes after reaction with atropine, possibly increasing the size of the molecule. As such, it was vital to explore the potential mechanism of this reaction to fully understand the possible implications within the sensing platform.

3.3. *Mechanistic insights of the bromocresol green and atropine interaction*

The electrochemical behaviour of atropine and bromocresol green was next investigated using both differential pulse voltammetry and square-wave voltammetry (Figure S8). The parameters were optimized for current intensity and peak width at half height, with the best conditions found using a 50 mV amplitude and 10 mV step potential, with a modulation time of 50 ms and a time interval of 0.5 s, for differential pulse voltammetry, and a frequency of 10 Hz, for square-wave voltammetry. As shown in Figure S8a and S8b, square-wave voltammetry was further selected due to its better defined voltammetric profile and higher peak currents.

The electrochemical response of atropine, before and after the colorimetric reaction with bromocresol green, is presented in Fig. 2a. The inset shows the visual result of the colorimetric reaction, with the colour transition from yellow (negative control) to green (positive test) upon atropine addition. In the presence of bromocresol green, the oxidation peak of atropine (P_{ATP}) decreased in current (magenta line), compared to atropine alone (red line), while bromocresol green processes (R_1 and O_2) exhibited increased peak currents in the presence of atropine versus bromocresol green alone (blue line). This indicates a chemical interaction between atropine and bromocresol green, likely consuming atropine and modifying the electrochemical behaviour of both species.

Bromocresol green exists in two major forms depending on pH, corresponding to yellow (− negative control, deprotonated) and green (+ positive test, protonated) colours (inset Fig. 2a), governed by the acid-base equilibrium illustrated in Fig. 2b. NMR characterization of bromocresol green in methanol (yellow form) showed that the aromatic protons (^1H) of the benzene ring, condensed with the cyclic sulfonate ester (compound 1), which were promptly attributed in the ^1H NMR spectrum (Fig. 2c (iv) – yellow). Notably, only one signal at 7.4 ppm (Hb in the yellow spectrum) is observed for the single aromatic proton present in both bromophenol derivative rings, confirming their similar chemical environments. However, in the presence of atropine (green form), the aromatic ^1H signals of bromocresol green exhibited significant chemical shift changes (Fig. 2c (ii) – green). Interestingly, the

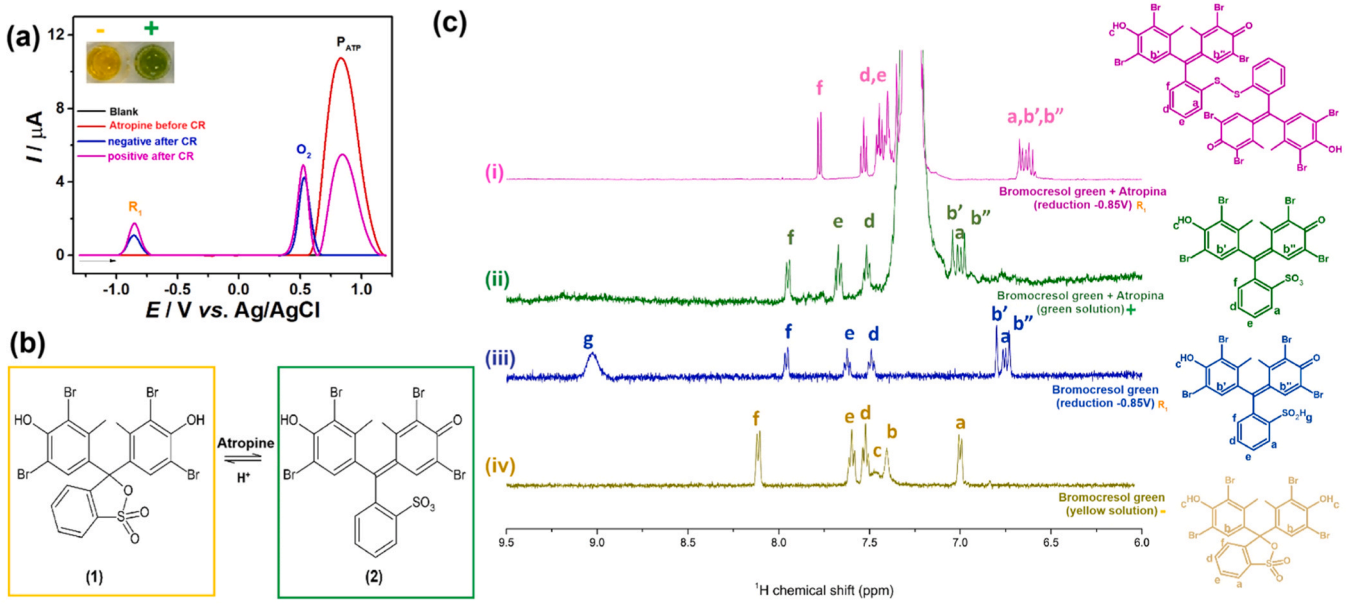

Fig. 2. (**a**) Square-wave voltammograms of pH 9 borate buffer before (blank: black line) and after addition of 0.5 mg mL^{-1} atropine (red line); and bromocresol green in absence (blue line) and in presence (magenta line) of atropine after colorimetric reaction (dilution x10), on a SPE-Gr. All potential scans started at −1.2 V. Experimental conditions: amplitude of 50 mV, step potential of 10 mV, and frequency 10 Hz. Inserted negative (yellow) and positive (green) results of the colorimetric test for atropine using bromocresol green. (**b**) Acid-base equilibrium of bromocresol green dye in the presence of atropine. (**c**) 1 H NMR superposition of bromocresol green in absence (iv – yellow spectrum) and in presence of atropine (ii – green spectrum), bromocresol green reduced product (R_1 - after electrolysis) (iii – blue spectrum), bromocresol green / atropine solution (1:12, mol:mol) and bromocresol green reduced product (R_1 - after electrolysis) in the presence of atropine (i – magenta spectrum).

phenolic hydrogen signal disappears, and two distinct chemical shifts are noted for the aromatic hydrogens of the Br-containing aromatic rings (Hb' and Hb''), which is consistent with a mesomeric effect (compound 2). This reaction was further confirmed by analysing the positive solution (green form) after the addition of acid (HCl), which caused it to revert to a yellow colour. The NMR spectrum once again demonstrated the presence of compound 1 (yellow form) along with an additional peak corresponding to atropine (Figure S9).

^{1}H NMR spectra after 4 h of electrolysis at −0.85 V (R_1) revealed structural changes in bromocresol green (blue spectra) and its mixture with atropine (magenta spectra), shown in Fig. 2c. Additionally, ^{1}H NMR spectra collected after 4 hours of continuous electrolysis at + 0.86 V for atropine (red spectra) are presented in Figure S10, illustrating the product formed following the P_{ATP} oxidation process.

The ^{1}H spectrum of the reduced product from bromocresol green (R_1) shows a chemical shift pattern indicative of the opened sulfonic ester ring, including two different chemical shifts for the aromatic hydrogens Hb' and Hb'' (Fig. 2c (iii) – blue). The higher chemical shift of the Hb hydrogens, along with the presence of an additional proton at 9.1 ppm, suggests the reduction of the sulfonic acid group (SO_3H – pKa 6.5 [38]) to a sulfinic acid group ($PhSO_2H$ – pKa 2.76 [39]). Interestingly, significant changes are noted for the reduced bromocresol green product (R_1) in the presence of atropine, where a complex spin system is observed for the ^{1}H aromatic signals (Fig. 2c (i) – magenta). This is in agreement with the larger diffusion coefficient obtained for this process in the presence of atropine described above. These results suggest the occurrence of dimerisation due to the reduction of the sulfonic (-SO_3) to thiol (-SH) group, and consequently, the formation of a disulfide bridge between two bromocresol green molecules.

Finally, the ^{1}H and ^{13}C spectra of atropine and its electro-oxidised product (P_{ATP}) are shown in Figure S10. Unlike previously reports [24, 40], the oxidation at + 0.85 V (*vs.* Ag/AgCl) does not lead to either an iminium ion intermediate or a noratropine product. The hydrogens (Hm at 2.75 ppm) and carbon (C11 at 39.7 ppm) of the tertiary amine are present in the NMR spectra remain intact. Instead, significant shifts are noted for ^{13}C nuclei at positions 7 and 10, suggesting structural modifications at those positions. Once mechanistically understood, it is important to relate this back to the square-wave voltammetry analytical response. A schematic overview of the proposed electrochemical reactions for atropine, bromocresol green, and their mixture is presented in Scheme 2.

Scheme 2 shown atropine exhibits an oxidation process (P_{ATP}) characterized by a two-electron and two-proton step, in which the anodic oxidation of hydroxyl occurs to form an aldehyde group. The structure of bromocresol green reduction involved in the mechanism is primarily related to the sulfonic ester group. The cathodic reduction of sulfur consists of a two-electron and a chemical elimination of water after the electron transfer, resulting in a sulfinic acid group. Nevertheless, bromocresol green reduction at −0.85 V in the presence of atropine lead a dimerization process through a disulfide bound as a result of a five -electron step.

3.4. *Dual detection of atropine before and after colorimetric reaction with bromocresol green*

Within the proposed sensing platform, the presence of atropine in the sample is confirmed, first, by the colour change (yellow to green – compound 1–2) in the colorimetric reaction with bromocresol green, and second, with the appearance of the oxidation peak for atropine at + 0.84 V *vs.* Ag/AgCl, as well as the increase in the characteristic peaks of bromocresol green (R_1 and O_2) after the colorimetric reaction. These two types of responses obtained show the potential for this approach in the selective, robust, and rapid identification of atropine. Repeatability (intra-electrode, N = 3) and reproducibility (inter-electrode, N = 5) studies were then performed with a concentration of 0.5 mg mL^{-1} of atropine before and after the colorimetric reaction, summarised in Table S3. These showed good stability for electrochemical responses of atropine before and after colorimetric reaction (P_{ATP}) as well as for bromocresol green redox processes (R_1 and O_2), with low relative standard deviations (RSDs) for the measurements of E_p (< 1 %) and I_p (<

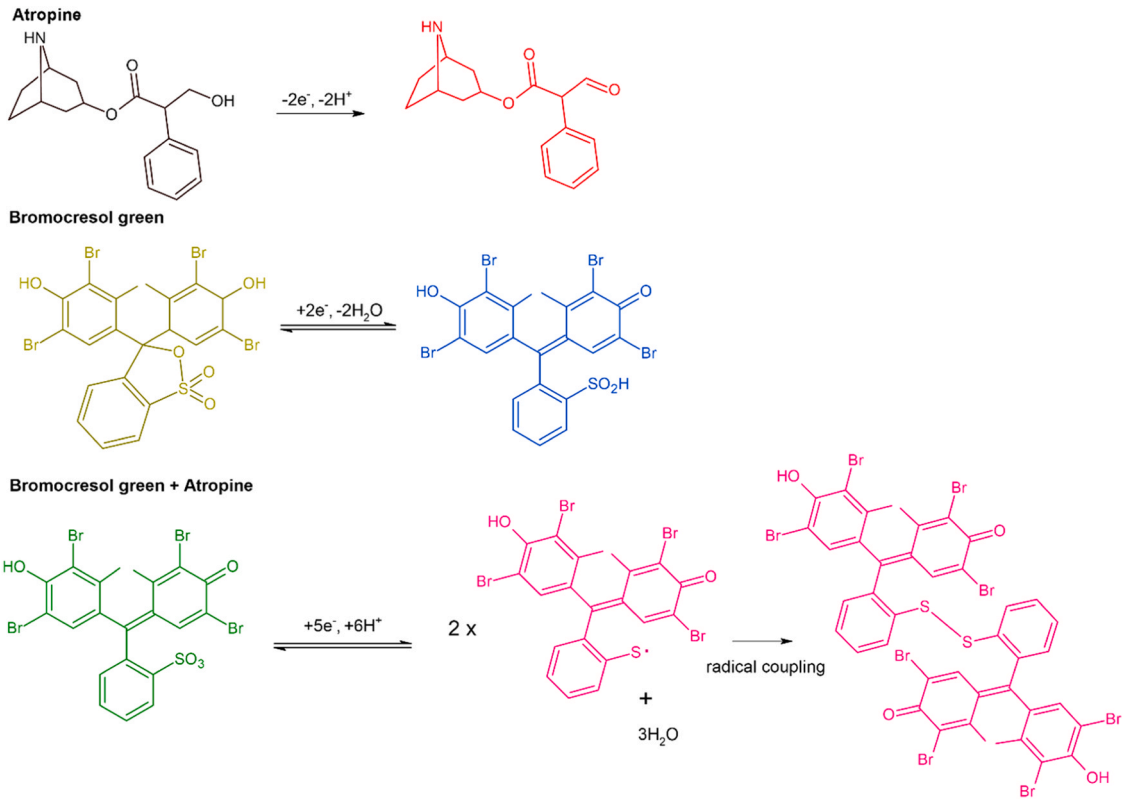

Scheme 2. Proposed electrochemical redox mechanism of atropine, bromocresol green and bromocresol green + atropine mixture using a SPE-Gr electrode at pH 9.

7 %). As shown in Table S3, the E_p of atropine was consistent across all measurements (RSDs < 0.8 %), making this an attractive screening method for identifying this molecule.

The optimal linear range for atropine determination by square-wave voltammetry before the colorimetric reaction was evaluated using standard solutions from 0.001 – 0.5 mg mL^{-1} (Fig. 3), where a good linearity (R^2 0.995) was observed up to 0.4 mg mL^{-1} of atropine (inset Fig. 3). Similarly, the linear range for atropine determination by square-wave voltammetry (after the colorimetric reaction) was evaluated using standard solutions of this analyte from 0.01 to 5.0 mg mL^{-1} for the colorimetric test and diluted ten-fold for electrochemical analysis (0.001 – 0.5 mg mL^{-1}), as depicted in Fig. 4. The potential window has been divided and presented separately in Figs. 4b and 4c) to facilitate visualisation of the processes, as the figure contains extensive information and multiple peaks from the same scan. It is important to note, however, that this data is acquired in a single scan from −1.2 V to + 1.2 V.

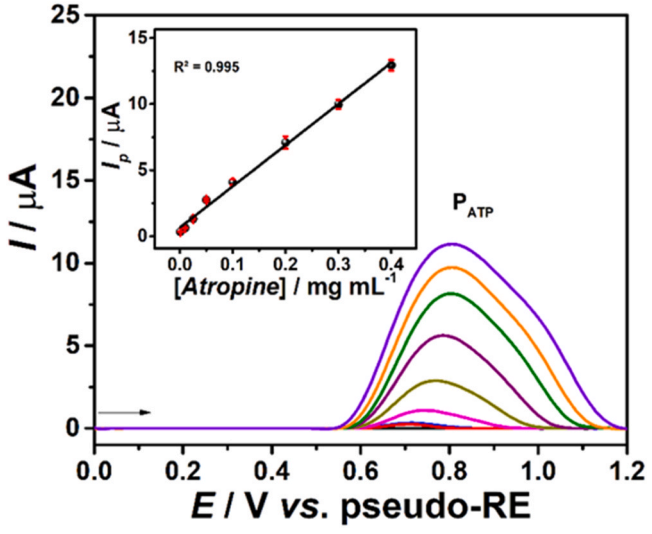

Fig. 3. square-wave voltammograms in pH 9 borate buffer on SPE-Gr after addition of 0.001–0.5 mg mL^{-1} atropine (black line represents blank solution response) before colorimetric reaction. The experimental conditions were the same as in Fig. 2a. Inset show linear regression. All measurements were performed in triplicate and the error bars (red) were smaller than the symbol (black) presented in the inset.

As can be seen in Fig. 4a, while the lowest concentration detectable by the colorimetric technique was 0.75 mg mL^{-1}, the lowest value detectable by square-wave voltammetry was 0.001 mg mL^{-1} (Fig. 3 and Fig. 4c), highlighting the difference in sensitivity obtained for both approaches. It is worth noting that all observed redox processes, after the colorimetric reaction between atropine and bromocresol green, can be used to quantify atropine in solution. Furthermore, linear regressions demonstrate that the lowest quantifiable value of atropine after the colorimetric reaction using square-wave voltammetry was 0.001 mg mL^{-1} for P_{ATP} and O_2, and 0.05 mg mL^{-1} for R_1 (Figs. 4b and 4c). These solutions were diluted and analysed using the electrochemical method, which showed linearity between 0.001 – 0.4 mg mL^{-1} and between 0.05 – 0.4 mg mL^{-1}. The linear regressions are presented in Table S4. It is worth mentioning that a wide range of low concentrations (0.01 – 5 mg mL^{-1}) was studied for the colorimetric test, although atropine causes damage to the human body in doses greater than 10 mg [7,41], demonstrating that the proposed method has sufficient sensitivity for detection in real samples of forensic interest – like spiked drinks.

The theoretical limit of detection (LOD) of 0.26 µg mL^{-1} was obtained using the equation $3S_B/m$ [42], where S_B is the standard deviation (N = 10) of the blank response and m is the slope of the calibration curve. The limit of quantification (LOQ) of 0.85 µg mL^{-1} was obtained using the equation $10S_B/m$ [42]. These values obtained before the colorimetric reaction are slightly lower than the LOD and LOQ values of 0.30 µg mL^{-1} and 1.00 µg mL^{-1} obtained after the colorimetric

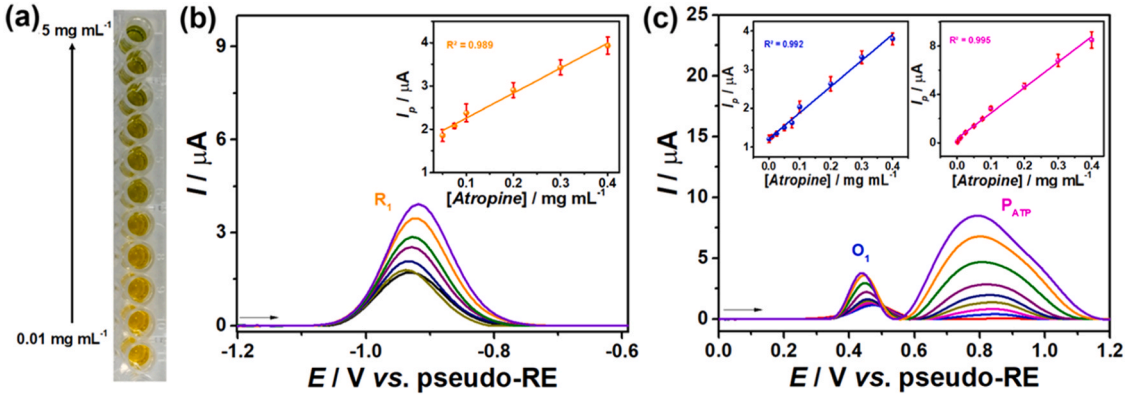

Fig. 4. (**a**) Results of the colorimetric test for atropine solutions in concentrations from 0.01 to 5.0 mg mL^{-1} and (**b** and **c**) square-wave voltammograms of these solutions diluted × 10 in 0.05 mol L^{-1} borate pH 9. Inserted linear regressions I_p vs. [atropine], R_1 in orange, O_2 in blue and P_{ATP} in magenta. All measurements were performed in triplicate and the error bars (red) were smaller than the symbol presented in the inset. The experimental conditions were the same as in Fig. 2a.

reaction. Furthermore, the lowest measurable value obtained for P_{ATP} (before and after the colorimetric reaction) and O_2 was 1.00 µg mL^{-1} (Figs. 3 and 4). The concentration levels detected for atropine are low enough for application in real samples (> 10 mg in beverages doped or > 1 µg mL^{-1} in urine [7,41]) using the proposed colorimetric-electrochemical method. Thus, the developed method is highly sensitive for screening atropine, employing a combination of colorimetric and electrochemical tests with quantification potential for this compound.

3.5. Interference studies

The ultimate application of the proposed dual methodology will be carried out in biological and beverage samples with special forensic interest. Therefore, interference studies were first carried out to investigate the influence of additional compounds for the reliable identification of atropine using the proposed method. The square-wave voltammetry results obtained from these interference studies are shown separately for UA, CA, AA, CAF, GLU and FRU, before and after the colorimetric reaction, in Figs. 5a and 5c, respectively. The result of the colorimetric tests is shown in Fig. 5b, always compared to the result of the blank (methanol – negative control "i").

It can be seen that only UA and AA showed redox processes under the conditions of the proposed method, both before (Fig. 5a) and after the colorimetric reaction (Fig. 5c). On the other hand, Fig. 5b demonstrates that the colorimetric step is highly selective for atropine compared to other compounds, as only in the presence of atropine the colour changed to green. Furthermore, Fig. 5c shows that the oxidation processes observed for AA and UA are close to the peak potential of atropine. Therefore, solutions mixing these substances with atropine in a 1:1 ratio were also evaluated, as shown in Figure S11. Even in these cases selective identification is possible using the proposed colorimetric-electrochemical method. It is also worth highlighting that only in the presence of atropine, a simultaneous increase in the R_1 peak current (at −1.0 V *vs.* Ag/AgCl) is observed (Fig. 5c), which can be also used for an indirect identification of atropine increasing the selectivity of the proposed methodology.

These studies demonstrated that the E_p of P_{ATP} remains practically unchanged (RSD <1 %), indicating that even in mixtures with other substances, such as AA and UA, there is no interference with the detection and quantification of atropine. Therefore, by using the oxidation signals P_{ATP} and R_1 in conjunction with the response from the colorimetric test, the proposed method provides a visual means of discriminating atropine in the presence of all tested substances without the need for a complex approach.

3.6. Determination of atropine in samples of forensic interest

Five drink samples (gin, tonic water, gin with tonic water, whisky, and energy drink) were spiked and evaluated using the proposed method

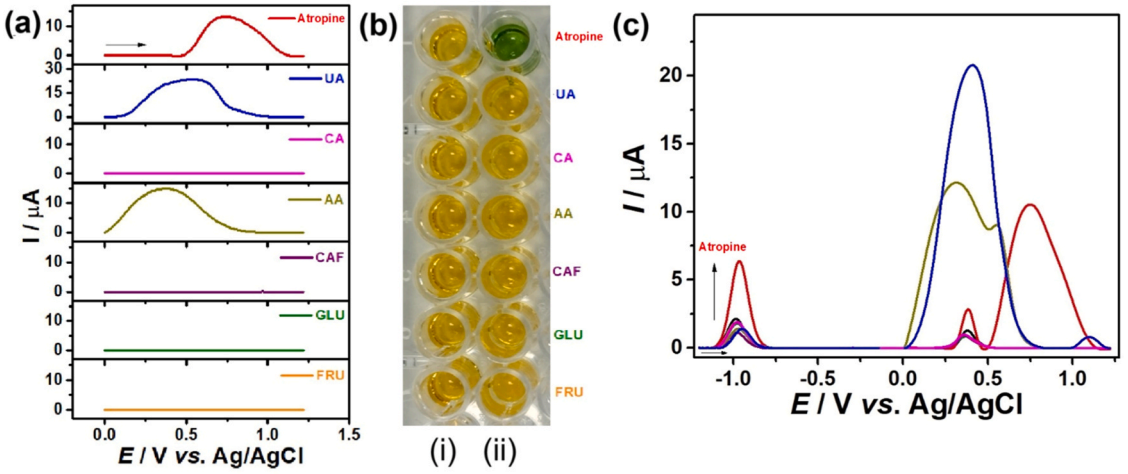

Fig. 5. Square-wave voltammograms before (**a**) and after (**c**) colorimetric reaction on SPE-Gr. Atropine (red line), UA (blue line), CA (magenta line), AA (dark yellow line), CAF (purple line), GLU (olive line) and FRU (orange line). All compounds were at a concentration of pH 9 borate buffer solution. The experimental conditions were the same as in Fig. 2a. (**b**) Results of the colorimetric test: (i) – blank and (ii) – atropine, UA, CA, AA, CAF, GLU and FRU, all at 5.0 mg mL^{-1}.

to identify atropine (Fig. 6 and Figure S12). Biological samples of synthetic urine, artificial saliva, and artificial vitreous humour spiked with atropine were also evaluated (Figs. 6d, 6e and Fig. 6f). All samples were spiked with 2.5 mg mL^{-1} atropine for the colorimetric test and diluted 10-times in borate buffer solution for the electro-chemical analysis. The presence of atropine in low concentrations in the different matrices analysed (Fig. 6 insets and Figure S12) was confirmed by the colour change (colorimetric step) and electrochemical profile similar to the standard of these substances in borate buffer solution (before and after the colorimetric reaction).

As can be seen in Figure S12, the colour change and electrochemical behaviour of atropine in the whisky and energy drink samples were similar to that of the standard for this substance. The colour change in the colorimetric test for atropine in tonic water and gin with tonic water is very subtle (Fig. 6b and Fig. 6c). Furthermore, tonic water samples present an oxidation process with an E_p close to P_{ATP}, causing an overlap of peak potential and compromising identification by this redox process. However, indirect atropine identification is possible by using the increase in I_p that occurs for R_1 only when atropine is present in the sample. For gin sample with tonic water (Fig. 6c), P_{ATP} can be clearly observed in the electrochemical stage despite the presence of quinine, probably because the proportion of tonic water is still lower and does not interfere with the analyses. Therefore, the proposed method using colorimetric and electrochemistry achieves atropine discrimination even in tonic water samples, which has been a major challenge in the preliminary identification of this substance in beverage samples of forensic interest. It is also worth noting that the atropine concentration evaluated is well below the concentration considered to posing a risk to human health. When risk concentration was studied, the colour changed to green in the atropine presence in all matrices was clearly seen.

Fig. 6d-f demonstrates that the electrochemical behaviour of atropine in biological samples was consistent with the standard behaviour of this substance. Therefore, the proposed method can be used effectively to identify atropine in saliva, urine, and vitreous humour (VH) samples using the colorimetric result (colour change to green), the appearance of P_{ATP}, and monitoring the increase in I_p of R_1. It is worth noting that for the VH matrix, the colorimetric test showed a blue colour (Fig. 6f) in the negative control (VH in the absence of atropine). Despite this different behaviour from other matrices evaluated, the colour change to green when atropine is present was easily observed in VH. Therefore, the proposed method is efficient in identifying atropine in biological samples.

As shown in Fig. 6, Figure S12 and Figure S13, the samples (both drinks and biological) exhibited the same electrochemical profile of atropine with P_{ATP} at its expected peak potential, indicating the presence of this substance in these samples. Only tonic water has been shown to have a potential for interference with atropine detection; however, indirect identification and quantification can be achieved using the increase in R_1, which only occurs when atropine is present. Furthermore, addition-recovery studies were carried out on these samples to evaluate the matrix effects for the detection and quantification of atropine. These results are shown in Table 1.

As can be seen in Table 1, in all matrices studied (drinks and biological), it is possible to quantify atropine using P_{ATP}, with recoveries between 93.9 (± 0.7) and 108.0 (± 0.9)%. It is worth noting that the other processes are used qualitatively, and that in the current forensic scenario, the primary interest in screening tests is selective identification, without the need to quantify the substance in the samples. Even so, the proposed method provides an interesting alternative to be used in situ as a rapid, simple, and selective screening test for the identification and quantification of atropine in forensic samples.

Table S5 – SI presents a comparison of the main analytical parameters for the determination of atropine using previously reported voltammetric methods. As shown in Table S5, the proposed method offers a

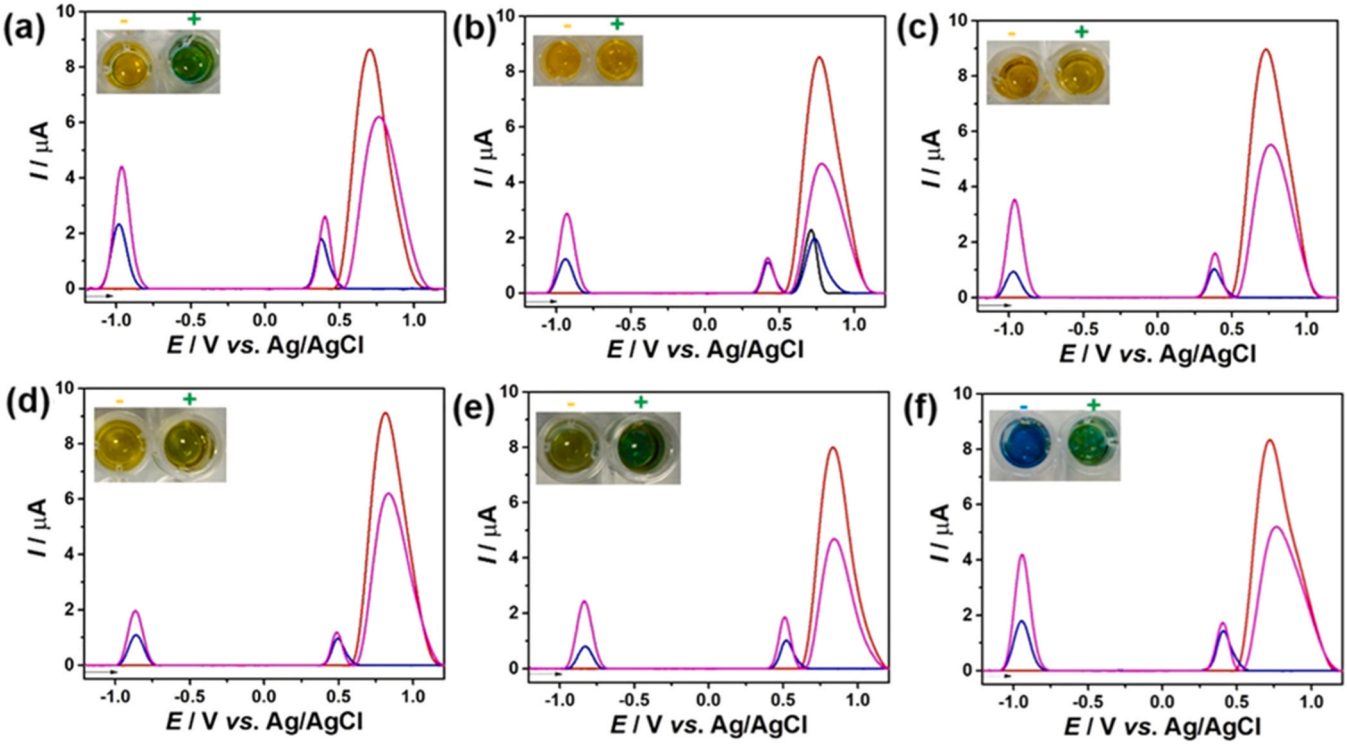

Fig. 6. Square-wave voltammograms recorded in pH 9 borate buffer solution before (black line) and after addition of 0.25 mg mL^{-1} atropine (red line), bromocresol green in absence (blue line) and in presence (magenta line) of atropine after colorimetric reaction (dilution x10), on a SPE-Gr. Atropine in gin (**a**), tonic water (**b**), gin with tonic water (**c**), artificial saliva (**d**), synthetic urine (**e**), and artificial vitreous humour (VH) (**f**). All potential scans started at −1.2 V. The experimental conditions were the same as in Fig. 2a. Insets: negative (yellow or blue – VH) and positive (green) results of the colorimetric test for atropine using bromocresol green within the real samples tested.

Table 1
Recovery (± RSD) for I_p of 0.25 mg mL^{-1} atropine in pH 9 borate buffer solution before and after colorimetric reaction, for drink and biological samples.

Matrix		Recovery % (I_p)			
		Before colorimetric reaction	After colorimetric reaction		
Drink		P_{ATP}	R_1	O_2	P_{ATP}
	Gin	102.3 (± 0.8)	90.1 (± 3.8)	90.1 (± 4.7)	106.5 (± 6.6)
	Whisky	93.9 (± 0.7)	104.5 (± 4.4)	125.8 (± 7.4)	71.7 (± 3.8)
	Tonic water	100.9 (± 0.8)	92.5 (± 3.9)	106.2 (± 5.6)	83.2 (± 5.2)
	Energy drink	101.4 (± 0.8)	96.7 (± 4.0)	123.7 (± 6.4)	97.3 (± 6.1)
	Gin with tonic water	106.2 (± 0.8)	113.4 (± 4.8)	134.7 (± 7.0)	98.3 (± 6.1)
Biological	Artificial Saliva	108.0 (± 0.9)	67.9 (± 2.6)	99.6 (± 5.2)	106.4 (± 6.6)
	Synthetic Urine	94.8 (± 0.7)	91.0 (± 3.3)	134.9 (± 8.2)	83.5 (± 5.2)
	Artificial VH	98.7 (± 0.8)	85.8 (± 3.6)	139.8 (± 7.6)	92.7 (± 5.7)

wide linear detection range compared to other methods. Additionally, it achieves a LOD than another unmodified screen-printed electrode (SPE)-based electroanalytical method. In contrast, extremely low LODs have been reported using electrodes modified with Co_3O_4-rGO, Chitosan-SWCNTs-GC, or GSH-Co_3O_4-GC. However, although these approaches provide greater sensitivity than the proposed method, the modified electrodes are more complex and less suitable for routine on-site forensic analysis.

Furthermore, unlike previously reported methods, the approach proposed here provides three distinct analytical responses by combining electrochemical and colorimetric techniques. In forensic analysis, multiple analytical methods are often required to support the issuance of official reports. This integrated approach offers more robust and reliable detection, contributing both to the preparation of expert evidence and to the immediate medical response for victims of atropine poisoning. Notably, it also enables the detection of atropine in the presence of tonic water — an interference that prevents detection when using electrochemical methods alone [9]. Given that tonic water has been frequently associated with gin to mask the taste of atropine in criminal cases, the ability to overcome this matrix effect is particularly relevant [9]. Only through this combined strategy is it possible to achieve the necessary selectivity and sensitivity for real-world applications in complex samples: initial electrochemical screening indicates the presence of atropine, the colorimetric change visually corroborates it, and the post-colorimetric electrochemical analysis confirms its presence—even in challenging matrices like tonic water.

4. Conclusions

In this study, we present a dual colorimetric-electrochemical platform that establishes a robust analytical basis for generating accurate forensic reports on suspected atropine use. The synergistic combination of colorimetric and electrochemical approaches facilitates the sensitive, simple, rapid, efficient, and reproducible detection and quantification of atropine in forensic contexts. Using an SPE-Gr with square-wave voltammetry for the rapid and sensitive detection of atropine in beverage and biological samples, a LOD of 0.255 μg mL^{-1} was achieved. This approach is primarily based on the electrochemical response of atropine before the colorimetric reaction, analysis of atropine -induced colour change in the colorimetric test using bromocresol green, followed by electrochemical analysis of the same solution. Detailed NMR analyses revealed that the reaction between bromocresol green and atropine is characterized by significant chemical shift changes in the aromatic hydrogen signals of bromocresol green, indicating a mesomeric effect and the formation of a dimer in the presence of atropine. Further-more, during electrochemical reduction, bromocresol green undergoes a transformation involving the opening of the sulfonate ester ring, forming a sulfinic acid group. In the presence of atropine, the reduced bromocresol green product (R_1) demonstrated evidence of dimerization due to the formation of a disulfide bridge between bromocresol green molecules, suggesting atropine's influence on the reaction dynamics. These findings highlight the complex interplay between bromocresol green and atropine, providing additional insights into the colorimetric and electrochemical processes underlying the detection mechanism. The method demonstrates reliability for forensic samples, showing good stability (RSD < 1 % for E_p and < 7 % for I_p) using the same or different SPE-Gr electrodes. It requires a small sample volume (45 μL) and simplifies sampling, improving portability and miniaturization for on-site analysis, which can be performed simultaneously using a portable potentiostat and a mobile phone. This innovative methodology overcomes the prevailing challenges in identifying and distinguishing atropine in beverage samples, particularly tonic water, where atropine can be identified indirectly through R_1. Furthermore, it contributes significantly to the judgment of forensic experts in a triage approach and assists in the preparation of comprehensive arrest reports.

CRediT authorship contribution statement

Bernalte Elena: Writing – review & editing, Writing – original draft, Supervision, Formal analysis, Conceptualization. **Crapnell Robert D.:** Writing – review & editing, Writing – original draft, Supervision, Investigation, Formal analysis. **Melo Larissa M. A.:** Writing – review & editing, Writing – original draft, Visualization, Validation, Methodology, Investigation, Formal analysis, Data curation. **Santos Wallans T. P.:** Writing – review & editing, Writing – original draft, Formal analysis. **Banks Craig E.:** Writing – review & editing, Writing – original draft, Visualization, Validation, Supervision, Software, Resources, Project administration, Methodology, Investigation, Funding acquisition, Formal analysis, Data curation, Conceptualization. **Verly Rodrigo M.:** Writing – review & editing, Writing – original draft, Formal analysis. **Muñoz Rodrigo A. A.:** Writing – review & editing, Writing – original draft, Supervision, Funding acquisition.

Declaration of Competing Interest

The authors declare that they have no known competing financial interests or personal relationships that could have appeared to influence the work reported in this paper.

Acknowledgements

The authors would like to thank Rizna Rizan and Tommy Whewell for their help in acquiring the MR data. The authors would like to acknowledge INCT-SP (CNPq/406958/ 2022–0, FAPEMIG/APQ-03984–24, and CAPES/88887.954256/2024–00, 88887.836030/2023–00 and Financial Code 001), CNPq (313367/2021–3), FAPEMIG [APQ-01996–23, RED-00120–23]. CAPES (88887.014930/2024–00) and Horizon Europe (grant 101137990) for their funding.

Appendix A. Supporting information

Supplementary data associated with this article can be found in the online version at doi:10.1016/j.snb.2025.137962.

Data availability

Data will be made available on request.

References

[1] K. Hillier, Atropine, in: S.J. Enna, D.B. Bylund (Eds.), xPharm: The Comprehensive Pharmacology Reference, Elsevier, New York, 2007, pp. 1–5.
[2] U.A. Eze, G.I. Nathaniel, G. Pepple, Ophthalmic uses of atropine: a review, J. Adv. Med. Med. Res. 34 (2022) 197–205.
[3] J.F. Lind, J.S. Crispin, D.K. McIver, The effect of atropine on the gastroesophageal sphincter, Can. J. Physiol. Pharmacol. 46 (1968) 233–238.
[4] I. Karunarathna, The role of atropine in modern medicine: indications, administration, and clinical outcomes, Uva Clin. (2024).
[5] P. Dauchot, J.S. Gravenstein, Effects of atropine on the electrocardiogram in different age groups, Clin. Pharmacol. Ther. 12 (1971) 274–280.
[6] M. Ahmed, D. Mridha, Unintentional jimson weed poisoning in a family: a case report, Cureus 15 (2023) e45604.
[7] L.J. DeFrates, J.D. Hoehns, E.L. Sakornbut, D.G. Glascock, A.R. Tew, Antimuscarinic intoxication resulting from the ingestion of moonflower seeds, Ann. Pharmacother. 39 (2005) 173–176.
[8] C.L. Winek, W.W. Wahba, C.L. Winek, T.W. Balzer, Drug and chemical blood-level data 2001, Forensic Sci. Int. 122 (2001) 107–123.
[9] R.D. Crapnell, C.E. Banks, Electroanalytical overview: the detection of the molecule of murder atropine, Talanta Open 4 (2021) 100073.
[10] H. Çaksen, D. Odabaş, S. Akbayram, Y. Cesur, Ş. Arslan, A. Üner, A.F. Öner, Deadly nightshade (Atropa belladonna) intoxication: an analysis of 49 children, Hum. Exp. Toxicol. 22 (2003) 665–668.
[11] S.L. Mohamed Adnane Berdai, Khadija Chetouani, Mustapha Harandou, Atropa belladonna intoxication: a case report, Pan Afr. Med. J. 11 (2012) 1937–8688.
[12] G. Heydenrych, Molecules of murder.criminal molecules and classical cases. By John Emsley, Angew. Chem. Int. Ed. 48 (2009), 2450-2450.
[13] P.A.M.M. Boermans, H.S. Go, A.M.A. Wessels, D.R.A. Uges, Quantification by HPLC-MS/MS of atropine in human serum and clinical presentation of six mild-to-moderate intoxicated atropine-adulterated-cocaine users, Ther. Drug Monit. 28 (2006).
[14] A.C. Gören, G. Bilsel, M. Bilsel, S. Yenisoy-Karakaş, D. Karakaş, Simple high-performance liquid chromatographic method for determination of atropine and obidoxime in a parenteral injection device, J. Chromatogr. A 1057 (2004) 237–239.
[15] G. Koželj, L. Perharič, L. Stanovnik, H. Prosen, Simple validated LC–MS/MS method for the determination of atropine and scopolamine in plasma for clinical and forensic toxicological purposes, J. Pharm. Biomed. Anal. 96 (2014) 197–206.
[16] M. Adams, M. Wiedenmann, G. Tittel, R. Bauer, HPLC-MS trace analysis of atropine in Lycium barbarum berries, Phytochem. Anal. 17 (2006) 279–283.
[17] F. Da Silva Santos, L. Vitor da Silva, P.V.S. Campos, C. de Medeiros Strunkis, C.M. G. Ribeiro, M.O. Salles, Review—recent advances of electrochemical techniques in food, energy, environment, and forensic applications, ECS Sens. 1 (2022) 013603.
[18] L. Shaw, L. Dennany, Applications of electrochemical sensors: forensic drug analysis, Curr. Opin. Electrochem. 3 (2017) 23–28.
[19] A. Florea, M. de Jong, K. De Wael, Electrochemical strategies for the detection of forensic drugs, Curr. Opin. Electrochem. 11 (2018) 34–40.
[20] I.V.S. Arantes, R.D. Crapnell, M.J. Whittingham, E. Sigley, T.R.L.C. Paixão, C. E. Banks, Additive manufacturing of a portable electrochemical sensor with a recycled conductive filament for the detection of atropine in spiked drink samples, ACS Appl. Eng. Mater. 1 (2023) 2397–2406.
[21] A. Zhang, C. Miao, H. Shi, H. Xiang, C. Huang, N. Jia, A novel solid-state electrochemiluminescence sensor for atropine determination based on Ru(bpy)32 + /carbon nanospheres/Nafion composite film, Sens. Actuators B: Chem. 222 (2016) 433–439.
[22] N.F. Atta, A. Galal, R.A. Ahmed, Direct and sensitive determination of atropine sulfate at polymer electrode in presence of surface active agents, Int. J. Electrochem. Sci. 7 (2012) 10365–10379.
[23] O. Ramdani, J.P. Metters, L.C.S. Figueiredo-Filho, O. Fatibello-Filho, C.E. Banks, Forensic electrochemistry: sensing the molecule of murder atropine, Analyst 138 (2013) 1053–1059.
[24] R.A. Dar, P.K. Brahman, S. Tiwari, K.S. Pitre, Electrochemical determination of atropine at multi-wall carbon nanotube electrode based on the enhancement effect of sodium dodecyl benzene sulfonate, Colloids Surf. B: Biointerfaces 91 (2012) 10–17.
[25] H. Bagheri, S.M. Arab, H. Khoshsafar, A. Afkhami, A novel sensor for sensitive determination of atropine based on a Co3O4-reduced graphene oxide modified carbon paste electrode, N. J. Chem. 39 (2015) 3875–3881.
[26] S. Mane, R. Narmawala, S. Chatterjee, Selective recognition of atropine in biological fluids and leaves of Datura stramonium employing a carbon nanotube–chitosan film based biosensor, N. J. Chem. 42 (2018) 10852–10860.
[27] A.F. João, R.G. Rocha, T.A. Matias, E.M. Richter, J. Flávio, S. Petruci, R.A. A. Muñoz, 3D-printing in forensic electrochemistry: atropine determination in beverages using an additively manufactured graphene-polylactic acid electrode, Microchem. J. 167 (2021) 106324.
[28] K. Torrarit, K. Promsuwan, A. Soleh, K. Saisahas, A. Thiagchanya, A. Phonchai, W. Limbut, Adsorptive anodic stripping voltammetric determination of atropine in urine sample, J. Electrochem. Soc. 168 (2021) 037512.
[29] R.W. Murray, A.G. Ewing, R.A. Durst, Chemically modified electrodes. Molecular design for electroanalysis, Anal. Chem. 59 (1987) 379A–390A.
[30] M.L. Wilson, K.A. Fleming, M.A. Kuti, L.M. Looi, N. Lago, K. Ru, Access to pathology and laboratory medicine services: a crucial gap, Lancet 391 (2018) 1927–1938.
[31] M.M.Ha.J.A. Siegel. Fundamentals of Forensic Science, Third ed., Elsevier, 2015.
[32] D. Nteziryayo, J. Wang, H. Qian, M. Liang, H. Liu, X. Liu, K. Uwantege, P. Joseph, Advancement and the existing landscape of forensic medicine in Africa: a comparison with developed countries, Forensic Sci., Med. Pathol. (2024).
[33] N. Bradbury, A Taste for Poison: Eleven deadly substances and the killers who used them HarperNorth2022.
[34] K. Brown, M. McMenemy, M. Palmer, M.J. Baker, D.W. Robinson, P. Allan, L. Dennany, Utilization of an electrochemiluminescence sensor for atropine determination in complex matrices, Anal. Chem. 91 (2019) 12369–12376.
[35] N. Laube, B. Mohr, A. Hesse, Laser-probe-based investigation of the evolution of particle size distributions of calcium oxalate particles formed in artificial urines, J. Cryst. Growth 233 (2001) 367–374.
[36] C. Qian, X. Wu, F. Zhang, W. Yu, Electrochemical impedance investigation of Ni-free Co-Cr-Mo and Co-Cr-Mo-Ni dental casting alloy for partial removable dental prosthesis frameworks, J. Prosthet. Dent. 116 (2016) 112–118.
[37] S.S. Thakur, S.K. Shenoy, J.S. Suk, J.S. Hanes, I.D. Rupenthal, Validation of hyaluronic acid-agar-based hydrogels as vitreous humor mimetics for in vitro drug and particle migration evaluations, Eur. J. Pharm. Biopharm. 148 (2020) 118–125.
[38] E.P.Sa.B. Dempsey, Ionization Constants of Organic Acids in Aqueous Solution, Elsevier Science & Technology, 1979.
[39] D. De Filippo, F. Momicchioli, A study of benzenesulfinic and seleninic acids: determination and theoretical interpretation of pK, Tetrahedron 25 (1969) 5733–5744.
[40] O. Dushna, L. Dubenska, M. Vojs, M. Marton, I. Patsay, S. Ivakh, S. Plotycya, Highly sensitive determination of atropine in pharmaceuticals, biological fluids and beverage on planar electrochemical cell with working boron-doped diamond electrode, Electrochim. Acta 432 (2022) 141182.
[41] S.R. Guharoy, M. Barajas, Atropine intoxication from the ingestion and smoking of jimson weed (Datura stramonium), Vet. Hum. Toxicol. 33 (1991) 588–589.
[42] A.M.B.J. Mocak, S. Mitchell, G. Scollary, A statistical overview of standard (IUPAC and ACS) and new procedures for determining the limits of detection and quantification: application to voltammetric and stripping techniques, Pure Appl. Chem. 69 (1997) 297–328.

Larissa M.A. Melo is a 3rd year PhD student in Chemistry at UFVJM, also holds a Master's degree in Analytical Chemistry, a Bachelor's degree in Chemical Engineering and Science and Technology, and a technical degree in Electrotechnics.

Elena Bernalte is a Senior Research Associate at MMU working in electrochemical sensing applications with special interest in additive manufacturing electrochemistry and sustainable electronics.

Robert D. Crapnell is the Technical Facility Manager for Electrochemistry & Polymer Science at MMU and works on the development of additive manufacturing electrochemistry and circular economy electrochemistry.

Rodrigo M. Verly is Associate Professor of Chemistry with expertise in synthesis, structural and conformational analysis of organic compounds, including biomolecules and nanobiostructures.

Rodrigo A.A. Munoz is Associate Professor of Chemistry, has published over 300 papers and works on the development of advanced electrochemical sensing technologies for real-time applications.

Wallans T.P. dos Santos is Professor of Chemistry and has published over 100 papers and works on electrochemistry and electroanalytical methods, notably for applications in forensic analysis and doping control.

Craig E. Banks holds a personal chair in chemistry and has published over 650 papers and works on next generation additive manufacturing electrochemical sensing platforms.